DOI Link: https://doi.org/10.61586/reNdh
Vol.43, Issue.5, Part.1, May 2025, PP.197-226

Mathematical Modelling and Bifurcation Analysis of Human-Mosquito Interactions for Malaria Control in Bangladesh

Sazia Khatun Tithi[1], Md Abdul Kuddus[1*], Azizur Rahman[2*], and Ashabul Hoque[1]

[1]Department of Mathematics, University of Rajshahi, Rajshahi 6205, Bangladesh.
[2]School of Computing, Mathematics and Engineering, Charles Sturt University, Wagga Wagga, NSW 2678, Australia.

*Corresponding authors: Md Abdul Kuddus, PhD; Azizur Rahman, PhD
e-mails: makuddus.math@ru.ac.bd; azrahman@csu.edu.au

Abstract

Malaria, an infectious disease caused by parasites and transmitted by Anopheles mosquitoes, affects individuals of all ages globally, including Bangladesh. In this work, we develop a transmission dynamics of malaria model between humans and mosquitoes and analyze its properties and solutions. Using the Next-Generation Matrix methods, our estimation of the fundamental reproduction number, R_0, shows that malaria spontaneously ends when R_0 is smaller than 1. On the other hand, malaria continues to exist within the populace if R_0 is larger than 1. We calibrate our proposed model with Bangladeshi malaria incidence data from 2010 to 2022 to estimate some model parameters. We also performed numerical analysis to support our analytic results and explored the impact of different parameters, finding that the infection dynamics are highly sensitive to variations in the transmission rates and the basic reproduction number, R_0. Specifically, when $R_0 < 1$, the disease tends to die out with lower levels of infected individuals in both human and mosquito populations, whereas for $R_0 > 1$, the infection spreads rapidly, leading to higher infection levels. Furthermore, higher human-to-mosquito transmission rates and loss of immunity significantly intensify the spread of malaria, emphasizing the need for targeted interventions. On the other hand, increased disease-related and recovery rates help reduce transmission. We used the sensitivity index to measure how the model's output changes in response to its input parameters. The results indicate that the rates of mosquito and human interaction significantly impact the prevalence of malaria. Finally, we performed a bifurcation analysis to explore the corresponding model parameters and demonstrated the stability of the situation. The findings of this analysis give policymakers guidance regarding the best course of action for reducing the burden of malaria in Bangladesh.

Keywords

Malaria model; Human and mosquito population; Stability and sensitivity analysis; Bifurcation analysis.

1. Introduction

Malaria affects over 300 million people in 90 countries worldwide, causing approximately one million deaths each year. By 2020, more than half the world's population was at risk of contracting malaria. In 2022, there were 249 million malaria infections globally, an increase of 16 million cases compared to the pre-pandemic figure of 233 million in 2019. The disease is transmitted by female Anopheles mosquitoes and can infect both humans and insects. Four species of the Plasmodium parasite cause malaria: *Plasmodium malariae, P. ovale, P. falciparum*, and *P. vivax*.According to the latest World Malaria Report, 29 million people were infected with malaria in 2022, up from 24 million in 2021. The estimated number of malaria-related deaths slightly decreased, from 610,000 in 2021 to 608,000 in 2022. Annually, between 100 and 400 million people are affected by malaria, out of the 2.5 billion at risk from *Plasmodium vivax* malaria [1, 2]. While the majority of cases and deaths occur in Sub-Saharan Africa, significant numbers are also reported in the Americas, Southeast Asia, the Eastern Mediterranean, and the Western Pacific, according to the World Health Organization (WHO).

Malaria is a common disease in tropical regions, with its local risk influenced by a combination of climatic, environmental, and societal factors. Climate conditions such as humidity, rainfall, and temperature significantly affect mosquito growth. Current research indicates that temperature plays a significant role in the spread of malaria in tropical and subtropical areas. According to Liu [3], extreme temperatures extend the lifespan of mosquitoes and shorten the time it takes for the malaria parasite to develop outside the mosquito. Rainy seasons create breeding habitats for mosquito eggs and support the growth of larvae that carry the disease [4]. Malaria manifests as an acute febrile illness. In people without immunity, symptoms generally appear 10-15 days after being bitten by an infected mosquito. Diagnosing malaria can be difficult since its initial symptoms, including fever, headache, and chills, are mild and not specific to the disease. As the disease progresses, symptoms can become more severe and include intense headaches, rashes, muscle and joint pain, and a fever that ranges from mild to incapacitating. In severe cases of Plasmodium vivax malaria, symptoms may include reduced consciousness, repeated seizures, extreme fatigue, abnormal bleeding, pulmonary edema (detectable via radiology), respiratory failure (acidotic breathing), and jaundice [5]. Currently, there is no specific treatment for malaria. The only effective way to prevent and manage the disease is through mosquito control or by preventing human-vector contact.

The World Health Organization (WHO) considers malaria a significant public health issue in Bangladesh. The Bangladeshi government tried to eliminate malaria in the 1960s, which nearly succeeded. Although the disease was nearly eradicated by the 1970s, it persisted in the eastern regions, particularly in areas with tea gardens and forests. However, the effort was abandoned during the

liberation struggle in 1971, leading to a resurgence of the disease. In response, the National Malaria Control Program (NMCP) was established in 1977 to control malaria. In the 1990s, malaria re-emerged as a major health concern, and it remains a serious issue today. Malaria transmission occurs mainly in Bangladesh's border areas for most of the year. Thirteen districts, primarily in the east and northeast of the country, lie in the high-risk malaria zone. These districts share borders with the Indian states of Assam, Tripura, and Meghalaya, as well as a part of Myanmar, with adults being the most impacted.

In 2002, there were 93 reported deaths, with a case fatality rate of 1.7% [6]. However, there were frequent instances of underreporting and misclassification of malaria cases. In 2006, routine laboratory surveillance in Bangladesh identified only 48,248 confirmed cases out of the roughly 2.9 million reported parasitic infections. Since 2007, NMCP efforts have accelerated significantly due to funding from the Global Fund, collaboration with academic and research institutions, and the support of a 21-member NGO consortium led by BRAC. Despite these efforts, by 2014, there were 57,480 confirmed malaria cases—almost double the number reported in 2013 [7]. The current malaria outbreak in the country is periodic and geographically concentrated. This situation highlights the need to study how specific malaria serotypes invade and survive in particular areas. Epidemiological models—both deterministic and stochastic—are valuable for analyzing the transmission dynamics of past outbreaks, such as those seen in the mid-20th century. Models like those developed by Tilahun et al. (2020) [8] use mathematical concepts to simulate real-world events and predict the severity of infectious diseases. These tools are crucial for policymakers, enabling them to evaluate health risks and gain a deeper understanding of disease transmission dynamics.

Various mathematical frameworks have been developed and analyzed to understand the spread of infectious diseases. One of the foundational contributions came from Kermack and McKendrick, who used a system of differential equations to describe disease transmission dynamics in their series of papers published in 1927 [7–11]. They introduced the concept of a threshold parameter that separates different dynamic regimes, with the idea that an infectious disease can only spread in a population if the basic reproduction number (R_0) exceeds a certain threshold. Mathematical models, due to their stronger computational predictive power, have proven to be more useful than statistical models for studying factors that influence the transmission of malaria [12–14]. These models can be informed by research findings and biological insights [15]. Different compartmentalized epidemiological models can be expressed using continuous modeling approaches, such as ordinary differential equations (ODEs), fractional differential equations (FDEs), and partial differential equations (PDEs) [16–19]. Modeling has become an essential tool in understanding malaria transmission dynamics, supporting control efforts, and identifying factors that influence the spread of the disease. For instance, Shikha [20] explored how population migration contributes to the rise in malaria cases.

She suggested employing SIS (susceptible-infectious-susceptible) and SIRS (susceptible-infectious-recovered-susceptible) epidemic models to study the scenario. In their study, Singh et al. (2005) applied the SIR (susceptible-infectious-recovered) model to analyze malaria transmission in Bangladesh. This approach allows a better understanding of how the disease spreads within the population and provides valuable insights for disease control and prevention efforts.

The spread of malaria in Bangladesh's cities can be estimated using mathematical models. These models enhance our understanding of genetic differences in infectious pathogens and the factors essential for diagnosis and treatment [21–27]. By defining the necessary criteria for disease elimination, mathematical models can also improve infectious disease surveillance and inform health policy [27–29]. Mathematical models play a crucial role in controlling malaria by identifying the extent of transmission and offering insights for epidemic control and prevention. They can help predict future outbreaks and enhance prevention strategies to avoid endemic diseases. Several factors, such as geographic expansion, increased transmission intensity in endemic regions, local climate variability, and habitat conditions, have contributed to a rise in malaria cases in Bangladesh. Combining pharmaceutical therapy with vector control is the most effective way to achieve a swift reduction in malaria cases. Doran et al. (2018) developed a malaria model that included these prevention strategies and performed a cost-effectiveness analysis [30]. To better understand malaria transmission in Bangladesh, Rahman et al. (2020) created a model showing that socioeconomic factors, such as education, play a critical role in developing and mitigating the disease [6]. Koutou et al. (2018) designed a malaria model to study global patterns of virus transmission and the vector-borne population, finding that the basic reproduction number (R_0) is key to understanding malaria dynamics in both endemic and epidemic stages [31].

Understanding the transmission dynamics of malaria is essential for devising effective control strategies. This study presents a mathematical model that incorporates non-linear infection rates, bifurcation analysis, and sensitivity analysis to provide insights into malaria control efforts. We developed and analyzed a human-mosquito malaria model consisting of two compartments for mosquitoes and three for humans. The model was examined both analytically and numerically from mathematical and biological perspectives. A key factor controlling the system's dynamics was identified, and the basic reproduction number was calculated using the next-generation matrix approach. We outlined the conditions under which malaria persists or is eradicated, emphasizing the model's behavior at different stages. To validate and support our analysis, we numerically solved the model's equations and studied the epidemic's trajectory across a range of plausible parameter values and initial conditions. First, we applied the Routh–Hurwitz criteria to assess the local stability of both endemic and disease-free equilibria. Next, we conducted a sensitivity analysis to determine the parameters that impact malaria prevalence most. Finally,

computational simulations and graphical interpretations were performed to examine the effects of key factors, including disease transmission rate, mortality rate, recovery rate, and immunity loss. Additionally, bifurcation analysis was conducted to gain a deeper understanding of the system's stability.

The structure of the paper is as follows: Sections 2 and 3 present the theoretical representation of the model, along with the necessary assumptions and solutions. Sections 4 and 5 cover the stability analysis and estimation of the model's parameters, respectively. Numerical simulations are provided in Section 6 to support the analytical findings. In Section 7, we carried out the bifurcation analysis. Sensitive analysis is performed in section 8. Finally, the model's results, discussion, and conclusion are presented in section 9.

2. Methods and Materials

We develop a compartmental model that classifies humans into susceptible, infectious, and recovered groups, while mosquitoes are categorized as susceptible and infectious. The model accounts for transmission dynamics, recovery, and immunity loss. The governing equations are derived using ordinary differential equations (ODEs) and incorporate biologically relevant parameters.

2.1. Model descriptions and analysis

Two mathematically deterministic models were developed: one for the human compartment, following a Susceptible–Infected–Recovered–Susceptible (SIRS) structure, and another for the mosquito compartment, following a Susceptible–Infected (SI) structure.

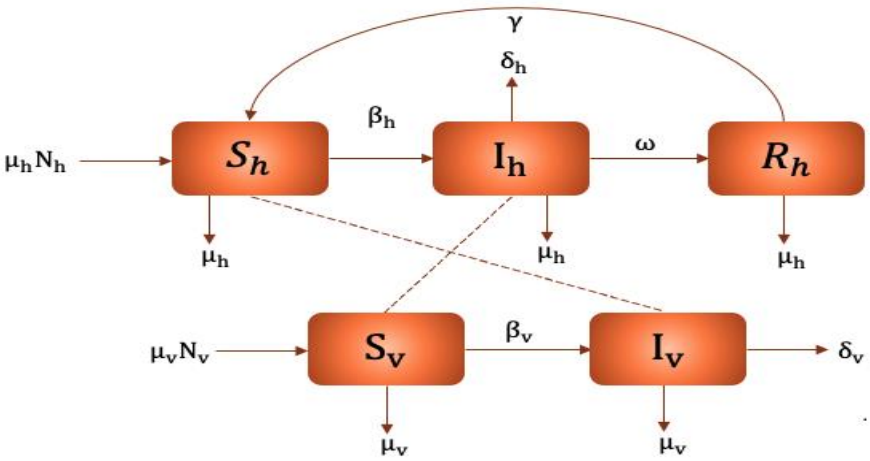

Fig. 1: A flow chart representing the computational representation of malaria.

The entire human population, represented by N_h (t), is divided by the model into the subsequent sub-classes: individuals with a higher risk of malaria S_h (t), those who exhibit symptoms of malaria I_h (t), and those who have recovered from malaria R_h (t). The entire number of people at any given moment t is specified as

$$N_h(t) = S_h(t) + I_h(t) + R_h(t), \quad (1)$$

which is said to be erratic, with people mixing at random. Susceptible mosquitoes (S_v) and infectious mosquitoes (I_v). make up the two subpopulations of the entire mosquito population, represented as $N_v(t)$. The mosquitoes have no recovered class and are always contagious [32, 33]. Therefore, at every given moment t, the overall number of mosquitoes in the population is provided by,

$$N_v(t) = S_v(t) + I_v(t), \quad (2)$$

Assumed in this instance is that a contagious female anopheles mosquito I_v (t), bites vulnerable people, S_h (t), and uses its beak to pierce the skin and inject a salivary enzyme that enters the circulation to keep the victim's blood from clotting. A fraction of those exposed develop active malaria and migrate at a rate of β_h to the affected human compartment I_h (t). On the other hand, the disease-related mortality rate for active malaria cases is δ_h. After a short period, the malaria cases that infected individuals recover at a pace of ω and move on to the section reserved for recovered participants R_h (t). The pace of loss of immunity causes an amount γ from the cured individuals' section R_h (t)to shift into the entirely susceptible human section S_h (t).

Concurrently, upon the bite of a contagious person by the vulnerable mosquito, S_v (t), with a likelihood β_v, the parasite combines with the mosquito, causing the mosquito to migrate from its susceptible compartment S_v (t) to the mosquito-infected chamber I_v (t). Nevertheless, δ_v is the disease-related death rate of the affected mosquito. Natural mortality occurs at a rate μ_h for human populations and $\mu_v$for mosquito populations. Figure 1 displays the model flow diagram.

The following two nonlinear ordinary equations describe the model, which derives the transmission of mosquito and human populations from the above:

$$\begin{cases} \frac{dS_h}{dt} = \mu_h N_h + \gamma R_h - \beta_h S_h I_v - \mu_h S_h \\ \frac{dI_h}{dt} = \beta_h S_h I_v - (\omega + \delta_h + \mu_h) I_h \\ \frac{dR_h}{dt} = \omega I_h - (\gamma + \mu_h) R_h \\ \frac{dS_v}{dt} = \mu_v N_v - \beta_v S_v I_h - \mu_v S_v \\ \frac{dI_v}{dt} = \beta_v S_v I_h - (\delta_v + \mu_v) I_v \end{cases} \quad (3)$$

Given the aforementioned system's non-negative beginning conditions:

$S_h(0) = S_{h0}, I_h(0) = I_{h0}, R_h(0) = R_{h0}, S_v(0) = S_{v0}, I_v(0) = I_{v0}$ for all t > 0.

With non-negative initial conditions, it is evident that all state variables will stay non-negative for t > 0. Furthermore, by summing Eqs. (3), we observe that the total population of humans, $N_h(t)$, and mosquitoes, $N_v(t)$, remain consistent over time

$\frac{dN_h}{dt} = 0$ and $\frac{dN_v}{dt} = 0$.

Integrating these equations, we find

N_h= constant and N_v = constant.

This shows that the total human and mosquito populations are constant and it naturally follows that each compartment states S_h, I_h, R_h and $S_v, I_v$are bounded.

2.2. Basic reproduction number

The model comprises three uninfected states $(S_h, R_h, \text{and } S_v)$and two infected states, (I_h, I_v). Despite the fact that the model has five states and a fluctuating overall population number. Since $I_h^0 = I_v^0 = R_h = 0$ at the disease-free steady state, $S_h = N_h$ and $S_v = N_v$. Only through N_h and N_v, either explicitly or implicitly, do the state variables S_h and S_v in Eq. (1) arise. S_h, S_v and $R_h$do not occur with other state variables as a result, (I_h, I_v), we have the following system:

$$\begin{cases} \frac{dI_h}{dt} = \beta_h S_h I_v - (\omega + \delta_h + \mu_h) I_h \\ \frac{dI_v}{dt} = \beta_v S_v I_h - (\delta_v + \mu_v) I_v \end{cases} \quad (4)$$

The differential equations (4) belong to the category of infectious subsystems since they solely account for creating new infections and modifying existing infections' states. Assuming that $X^T = (I_h, I_v)^T$, T stands for transposition, we should now express the infection subsystem as follows:

$$\dot{X} = (F + V)X. \quad (5)$$

The transmission matrix is represented by F, and transitions by matrix V. The matrices are obtained from the system of Equation (4) by separating the transmission events from other events. Concerning the afflicted states indicated

by indexes i and j, where i, j ∈ 1, 2, entry V_{ij} represents how frequently those residing in an infected state j procreate inside the system with humans in an infected state i. Thus, for Equation (4), we get

$$F = \begin{bmatrix} 0 & \beta_h S_h \\ \beta_v S_v & 0 \end{bmatrix}$$

and

$$V = \begin{bmatrix} -(\omega + \delta_h + \mu_h) & 0 \\ 0 & -(\delta_v + \mu_v) \end{bmatrix}$$

The next generation matrix, K, is presented in [10], with attention to the crucial negative sign,

$$K = -FV^{-1} = F(-V^{-1}) = \begin{pmatrix} 0 & \frac{S_h \beta_h}{\delta_v + \mu_v} \\ \frac{S_v \beta_v}{\omega + \delta_h + \mu_h} & 0 \end{pmatrix}$$

The fundamental reproduction numbers of malaria, or the median number of additional infections created by an infected individual, are represented by the dominating eigenvalues of K. Therefore, the fundamental reproduction number is

$$R_0 = \sqrt{\frac{N_h \mu_h \beta_h N_v \mu_v \beta_v}{(\delta_v + \mu_v)(\omega + \delta_h + \mu_h)}}. \quad (6)$$

In (6), $\frac{1}{(\omega_h + \delta_h + \mu_h)}$shows how long the human infectious phase usually lasts; $\frac{\mu_v}{(\delta_v + \mu_v)}$ is the likelihood that mosquitoes will remain exposed and spread the disease. Let R_0, the fundamental reproduction number, be expressed as

$$R_0 = \sqrt{R_{0h} R_{0v}} \quad (7)$$

where $R_{0h} = \frac{N_h \mu_h \beta_h}{(\omega + \delta_h + \mu_h)}$and $R_{0v} = \frac{N_v \mu_v \beta_v}{(\delta_v + \mu_v)}$

The total number of people in a fully susceptible human population that an infected mosquito infects throughout its expected infection period is represented by R_{0h} in this case, however, R_{0v} represents the entire number of mosquitoes within a susceptible population that contract an illness from a single infected person within the duration of the infection.

3. Model analysis

Here, we list the fundamental characteristics of the suggested malaria model (3).

3.1. Equilibrium analysis

This system yields two distinct types of equilibria. First, the disease-free equilibrium occurs when the basic reproduction number R_0 is less than one (i.e, $R_0 < 1$), indicating that the disease cannot sustain itself in the population. Conversely, when R_0 exceeds one (i.e., $R_0 > 1$), the system reaches an endemic equilibrium, signifying a stable presence of the disease. Importantly, a disease-free equilibrium always exists in the equations specified in (3)

$$E_0 = (S_{0h}, I_{0h}, R_{0h}, S_{0v}, I_{0v}) = (N_h, 0, 0, N_v, 0).$$

We may also determine the disease-endemic equilibrium from Equation (3)

$E^* = (S_h^*, I_h^*, R_h^*, S_v^*, I_v^*)$at which malaria continues to exist in populations of mosquitoes and humans:

$$\begin{cases} S_h^* = \frac{N_h \mu_h}{R_0^2}(\beta_v I_h^* + \mu_v) \\ I_h^* = N_h \mu_h \left(1 - \frac{\mu_h \mu_v}{R_0^2}\right)\left[\frac{\mu_h^2 N_h \beta_v}{R_0^2} + (\omega + \delta_h + \mu_h) - \frac{\gamma\omega}{\gamma+\mu_h}\right]^{-1} \\ R^* = \frac{\omega I_h^*}{\gamma+\mu_h} \\ S_v^* = \frac{\mu_v N_v}{\beta_v I_h^* + \mu_v} \\ I_v^* = \frac{\beta_v S_v I_h^*}{\delta_v+\mu_v} \end{cases} \quad (8)$$

According to Equation (8), in all of the above-mentioned components (S_h^*, R_h^*, S_v^*, I_v^*), getting $R_0 > 1$ is an adequate prerequisite for the non-negative status of the Indigenous community I_h^*. This is because the endemic equilibrium zone in which the criterion $I_h^* > 0$ needed $R_0 > 1$. Thus, Equation (3) has an endemic equilibrium $E^* = (S_h^*, I_h^*, R_h^*, S_v^*, I_v^*)$ if $R_0 > 1$.

4. Stability analysis

The equilibria of Equation (1) are investigated for stability, and the following findings are made.

4.1. Disease-free equilibrium

The model's disease-free equilibrium is analyzed using the Jacobian matrix and Routh-Hurwitz criteria, confirming local stability when $R_0 < 1$.

Lemma 1: $R_0 < 1$ indicates the local stability of the model's disease-free equilibrium, whereas $R_0 > 1$ indicates instability.

Proof: We derive the Jacobian matrix from Equation (3), which results in

$$J = \begin{pmatrix} -(\beta_h I_v + \mu_h) & 0 & \gamma & 0 & -\beta_h S_h \\ \beta_h I_v & -(\mu_h + \delta_h + \omega) & 0 & 0 & \beta_h S_h \\ 0 & \omega & -(\gamma + \mu_h) & 0 & 0 \\ 0 & -\beta_v S_v & 0 & -(\mu_v + \beta_v I_h) & 0 \\ 0 & \beta_v S_v & 0 & \beta_v I_h & -(\mu_v + \delta_v) \end{pmatrix}$$

which, at E_0, the equilibrium without illness, decreases to

$$J(E^0) = \begin{pmatrix} -\mu_h & 0 & \gamma & 0 & -\beta_h N_h \\ 0 & -(\mu_h + \delta_h + \omega) & 0 & 0 & \beta_h N_h \\ 0 & \omega & -(\gamma + \mu_h) & 0 & 0 \\ 0 & -\beta_v N_v & 0 & -\mu_v & 0 \\ 0 & \beta_v N_v & 0 & 0 & -(\mu_v + \delta_v) \end{pmatrix}$$

To confirm the stability of E^0, all eigenvalues of $J(E^0)$ must be shown to have negative real parts. Since in the first and fourth columns, only the diagonal elements are shown that makeup $-\mu_h$ and $-\mu_v$, the two negative eigenvalues. Similarly, the only diagonal term in $J(E^0)$'s third column is $-(\gamma + \mu_h)$, which is a negative eigenvalue. Using the corresponding characteristic equation, the next four eigenvalues are found:

$$(\lambda + \omega + \delta_h + \mu_h)(\lambda + \delta_v + \mu_v) - N_h N_v \beta_h \beta_v = 0 \quad (9)$$

Consider, $A_1 = \omega + \delta_h + \mu_h$ and $A_2 = \delta_v + \mu_v$, then (9) becomes

$$B_1\lambda + B_0 = 0 \quad (10)$$

where, $B_1 = (A_1 + A_2)$ and $B_0 = A_1A_2 - N_hN_v\beta_h\beta_v = A_1A_2 - S_hS_v\beta_h\beta_v$ (11)

Additionally, modifying B_0 in relation to R_0, the basic reproduction number produces,

$$B_0 = A_1A_2(1 - R_0^2) \quad (12)$$

The Routh-Hurwitz criteria [34, 35] is utilized, indicating that for i = 1, 2, every root of the polynomial (10) includes negative real portions if and only if all the coefficients $B_i$are positive as well as the matrices $H_i > 0$. It may be concluded that if $B_1 > 0$, then all A_i's are positive. Furthermore, (12) implies that $B_0 > 0$ if $R_0 < 1$. Moreover, it is revealed that the polynomial (10) has positive Hurwitz matrices.

That is, $H_1 = B_0 > 0$ and $H_2 = [B_0 \quad B_1] > 0$.

As a result, the disease-free equilibrium state is steadily stable locally, and every eigenvalue of the Jacobian equation matrix $J(E_0)$ has the negative real component when $R_0 < 1$. But when $R_0 > 1$, we observe that $B_0 < 1$, and according to Descartes's rule of terms [34], the arrangement of the polynomial's coefficients,B_1, B_0, changes by exactly one sign. Therefore, the equilibrium point free from sickness will be unstable if only one positive eigenvalue exists.

4.2. Disease endemic equilibrium

Lemma 2: Regional stability states that native equilibria E* are stable when $R_0 > 1$.

Proof: We compute the Jacobian matrix from the system of Equation (3) at E*, which results in

$$J = \begin{pmatrix} -(\beta_h I_v + \mu_h) & 0 & \gamma & 0 & -\beta_h S_h \\ \beta_h I_v & -(\mu_h + \delta_h + \omega) & 0 & 0 & \beta_h S_h \\ 0 & \omega & -(\gamma + \mu_h) & 0 & 0 \\ 0 & -\beta_v S_v & 0 & -(\mu_v + \beta_v I_h) & 0 \\ 0 & \beta_v S_v & 0 & \beta_v I_h & -(\mu_v + \delta_v) \end{pmatrix}$$

The equation for J* (E*) features is defined as follows:

$$|J^*(E^*) - \lambda I| = 0$$

$$\Rightarrow \begin{vmatrix} -(\beta_h I_v + \mu_h) - \lambda & 0 & \gamma & 0 & -\beta_h S_h \\ \beta_h I_v & -(\mu_h + \delta_h + \omega) - \lambda & 0 & 0 & \beta_h S_h \\ 0 & \omega & -(\gamma + \mu_h) - \lambda & 0 & 0 \\ 0 & -\beta_v S_v & 0 & -(\mu_v + \beta_v I_h) - \lambda & 0 \\ 0 & \beta_v S_v & 0 & \beta_v I_h & -(\mu_v + \delta_v) - \lambda \end{vmatrix} = 0$$

$$\Rightarrow \lambda^5 + P_1\lambda^4 + P_2\lambda^3 + P_3\lambda^2 + P_4\lambda + P_5 = 0 \quad (13)$$

where

$$P_1 = I_h\beta_v + I_v\beta_h + 2\mu_v + \delta_h + 3\mu_h + \omega + \delta_v + \gamma$$

$$\begin{aligned} P_2 = {} & I_h I_v \beta_h \beta_v - S_h S_v \beta_h \beta_v + I_h \mu_v \beta_v + I_h \delta_h \beta_v + 3 I_h \beta_v \mu_h + I_h \beta_v \omega + I_h \beta_v \delta_v \\ & + 2 I_v \mu_v \beta_h + I_v \beta_h \delta_h + 2 I_v \beta_h \mu_h + I_v \beta_h \omega + I_v \beta_h \delta_v + \gamma I_h \beta_v \\ & + \gamma I_v \beta_h + \mu_v^2 + 2\mu_v \delta_h + 6\mu_v \mu_h + 2\mu_v \omega + \mu_v \delta_v + 2\delta_h \mu_h \\ & + \delta_h \delta_v + 3\mu_h^2 + 2\mu_h \omega + 3\mu_h \delta_v + \omega \delta_v + 2\gamma \mu_v + \gamma \delta_h \\ & + 2\gamma \mu_h + \gamma \omega + \gamma \delta_v \end{aligned}$$

$$P_3 = I_h I_v \mu_v \beta_h \beta_v + I_h I_v \beta_h \delta_h \beta_v + 2I_h I_v \beta_h \beta_v \mu_h + I_h I_v \beta_h \beta_v \omega + I_h I_v \beta_h \beta_v \delta_v - S_h S_v \mu_v \beta_h \beta_v - 2S_h S_v \beta_h \beta_v \mu_h + \gamma I_h I_v \beta_h \beta_v + I_h \mu_v \delta_h \beta_v + 3I_h \mu_v \beta_v \mu_h + I_h \mu_v \beta_v \omega + 2I_h \delta_h \beta_v \mu_h + I_h \delta_h \beta_v \delta_v + 3I_h \beta_v \mu_h^2 + 2I_h \beta_v \mu_h \omega + 3I_h \beta_v \mu_h \delta_v + I_h \beta_v \omega \delta_v + I_v \mu_v^2 \beta_h + 2I_v \mu_v \beta_h \delta_h + 4I_v \mu_v \beta_h \mu_h + 2I_v \mu_v \beta_h \omega + I_v \mu_v \beta_h \delta_v + I_v \beta_h \delta_h \mu_h + I_v \beta_h \delta_h \delta_v + I_v \beta_h \mu_h^2 + I_v \beta_h \mu_h \omega + 2I_v \beta_h \mu_h \delta_v + I_v \beta_h \omega \delta_v - \gamma S_h S_v \beta_h \beta_v + \gamma I_h \mu_v \beta_v + \gamma I_h \delta_h \beta_v + 2\gamma I_h \beta_v \mu_h + \gamma I_h \beta_v \omega + \gamma I_h \beta_v \delta_v + 2\gamma I_v \mu_v \beta_h + \gamma I_v \beta_h \delta_h + \gamma I_v \beta_h \mu_h + \gamma I_v \beta_h \omega + \gamma I_v \beta_h \delta_v + \mu_v^2 \delta_h + 3\mu_v^2 \mu_h + \mu_v^2 \omega + 4\mu_v \delta_h \mu_h + \mu_v \delta_h \delta_v + 6\mu_v \mu_h^2 + 4\mu_v \mu_h \omega + 3\mu_v \mu_h \delta_v + \mu_v \omega \delta_v + \delta_h \mu_h^2 + 2\delta_h \mu_h \delta_v + \mu_h^3 + \mu_h^2 \omega + 3\mu_h^2 \delta_v + 2\mu_h \omega \delta_v + \gamma \mu_v^2 + 2\gamma \mu_v \delta_h + 4\gamma \mu_v \mu_h + 2\gamma \mu_v \omega + \gamma \mu_v \delta_v + \gamma \delta_h \mu_h + \gamma \delta_h \delta_v + \gamma \mu_h^2 + \gamma \mu_h \omega + 2\gamma \mu_h \delta_v + \gamma \omega \delta_v$$

$$P_4 = I_h I_v \mu_v \beta_h \delta_h \beta_v + 2I_h I_v \beta_h \beta_v \mu_h \mu_v + I_h I_v \mu_v \beta_h \beta_v \omega + I_h I_v \beta_h \delta_h \beta_v \mu_h + I_h I_v \beta_h \delta_h \beta_v \delta_v + I_h I_v \beta_h \beta_v \mu_h^2 + I_h I_v \beta_h \beta_v \mu_h \omega + 2I_h I_v \beta_h \beta_v \mu_h \delta_v + I_h I_v \beta_h \beta_v \omega \delta_v - 2S_h S_v \mu_v \beta_h \beta_v \mu_h - S_h S_v \beta_h \beta_v \mu_h^2 + \gamma I_h I_v \mu_v \beta_h \beta_v + \gamma I_h I_v \beta_h \delta_h \beta_v + \gamma I_h I_v \beta_h \beta_v \mu_h + \gamma I_h I_v \beta_h \beta_v \omega + \gamma I_h I_v \beta_h \beta_v \delta_v + 2I_h \mu_v \delta_h \beta_v \mu_h + 3I_h \mu_v \beta_v \mu_h^2 + 2I_h \mu_v \beta_v \mu_h \omega + I_h \delta_h \beta_v \mu_h^2 + 2I_h \delta_h \beta_v \mu_h \delta_v + I_h \beta_v \mu_h^3 + I_h \beta_v \mu_h^2 \omega + 3I_h \beta_v \mu_h^2 \delta_v + 2I_h \beta_v \mu_h \omega \delta_v + I_v \mu_v^2 \beta_h \delta_h + 2I_v \mu_v^2 \beta_h \mu_h + I_v \mu_v^2 \beta_h \omega + 2I_v \mu_v \beta_h \delta_h \mu_h + I_v \mu_v \beta_h \delta_h \delta_v + 2I_v \mu_v \beta_h \mu_h^2 + 2I_v \mu_v \beta_h \mu_h \omega + 2I_v \mu_v \beta_h \mu_h \delta_v + I_v \mu_v \beta_h \omega \delta_v + I_v \beta_h \delta_h \mu_h \delta_v + I_v \beta_h \mu_h^2 \delta_v + I_v \beta_h \mu_h \omega \delta_v - \gamma S_h S_v \mu_v \beta_h \beta_v - \gamma S_h S_v \beta_h \beta_v \mu_h + \gamma I_h \mu_v \delta_h \beta_v + 2\gamma I_h \mu_v \beta_v \mu_h + \gamma I_h \mu_v \beta_v \omega + \gamma I_h \delta_h \beta_v \mu_h + \gamma I_h \delta_h \beta_v \delta_v + \gamma I_h \beta_v \mu_h^2 + \gamma I_h \beta_v \mu_h \omega + 2\gamma I_h \beta_v \mu_h \delta_v + \gamma I_h \beta_v \omega \delta_v + \gamma I_v \mu_v^2 \beta_h + 2\gamma I_v \mu_v \beta_h \delta_h + 2\gamma I_v \mu_v \beta_h \mu_h + 2\gamma I_v \mu_v \beta_h \omega + \gamma I_v \mu_v \beta_h \delta_v + \gamma I_v \beta_h \delta_h \delta_v + \gamma I_v \beta_h \mu_h \delta_v + \gamma I_v \beta_h \omega \delta_v + 2\mu_v^2 \delta_h \mu_h + 3\mu_v^2 \mu_h^2 + 2\mu_v^2 \mu_h \omega + 2\mu_v \delta_h \mu_h^2 + 2\mu_v \delta_h \mu_h \delta_v + 2\mu_v \mu_h^3 + 2\mu_v \mu_h^2 \omega + 3\mu_v \mu_h^2 \delta_v + 2\mu_v \mu_h \omega \delta_v + \delta_h \mu_h^2 \delta_v + \mu_h^3 \delta_v + \mu_h^2 \omega \delta_v + \gamma \mu_v^2 \delta_h + 2\gamma \mu_v^2 \mu_h + \gamma \mu_v^2 \omega + 2\gamma \mu_v \delta_h \mu_h + \gamma \mu_v \delta_h \delta_v + 2\gamma \mu_v \mu_h^2 + 2\gamma \mu_v \mu_h \omega + 2\gamma \mu_v \mu_h \delta_v + \gamma \mu_v \omega \delta_v + \gamma \delta_h \mu_h \delta_v + \gamma a \mu_h^2 \delta_v + \gamma \mu_h \omega \delta_v$$

$$P_5 = I_h I_v \mu_v \beta_h \delta_h \beta_v \gamma + I_h I_v \mu_v \beta_h \delta_h \beta_v \mu_h + I_h I_v \mu_v \beta_h \beta_v \gamma \mu_h + I_h I_v \mu_v \beta_h \beta_v \gamma \omega + I_h I_v \mu_v \beta_h \beta_v \mu_h^2 + I_h I_v \mu_v \beta_h \beta_v \mu_h \omega + I_h I_v \beta_h \delta_h \beta_v \gamma \delta_v + I_h I_v \beta_h \delta_h \beta_v \mu_h \delta_v + I_h I_v \beta_h \beta_v \gamma \mu_h \delta_v + I_h I_v \beta_h \beta_v \gamma \omega \delta_v + I_h I_v \beta_h \beta_v \mu_h^2 \delta_v + I_h I_v \beta_h \beta_v \mu_h \omega \delta_v - S_h S_v \mu_v \beta_h \beta_v \gamma \mu_h - S_h S_v \mu_v \beta_h \beta_v \mu_h^2 + I_h \mu_v \delta_h \beta_v \gamma \mu_h + I_h \mu_v \delta_h \beta_v \mu_h^2 + I_h \mu_v \beta_v \gamma \mu_h^2 + I_h \mu_v \beta_v \gamma \mu_h \omega + I_h \mu_v \beta_v \mu_h^3 + I_h \mu_v \beta_v \mu_h^2 \omega + I_h \delta_h \beta_v \gamma \mu_h \delta_v + I_h \delta_h \beta_v \mu_h^2 \delta_v + I_h \beta_v \gamma \mu_h^2 \delta_v + I_h \beta_v \gamma \mu_h \omega \delta_v + I_h \beta_v \mu_h^3 \delta_v + I_h \beta_v \mu_h^2 \omega \delta_v + I_v \mu_v^2 \beta_h \delta_h \gamma + I_v \mu_v^2 \beta_h \delta_h \mu_h + I_v \mu_v^2 \beta_h \gamma \mu_h + I_v \mu_v^2 \beta_h \gamma \omega + I_v \mu_v^2 \beta_h \mu_h^2 + I_v \mu_v^2 \beta_h \mu_h \omega + I_v \mu_v \beta_h \delta_h \gamma \delta_v + I_v \mu_v \beta_h \delta_h \mu_h \delta_v + I_v \mu_v \beta_h \gamma \mu_h \delta_v + I_v \mu_v \beta_h \gamma \omega \delta_v + I_v \mu_v \beta_h \mu_h^2 \delta_v + I_v \mu_v \beta_h \mu_h \omega \delta_v + \mu_v^2 \delta_h \gamma \mu_h + \mu_v^2 \delta_h \mu_h^2 + \mu_v^2 \gamma \mu_h^2 + \mu_v^2 \gamma \mu_h \omega + \mu_v^2 \mu_h^3 + \mu_v^2 \mu_h^2 \omega + \mu_v \delta_h \gamma \mu_h \delta_v + \mu_v \mu_h^2 \delta_v + \mu_v \gamma \mu_h^2 \delta_v + \mu_v \gamma \mu_h \omega \delta_v + \mu_v \delta_h \gamma \mu_h \delta_v + \mu_v \gamma \mu_h^2 \delta_v + \mu_v \gamma \mu_h \omega \delta_v$$

Based on the above relations, we can analyze as follows:

$P_1 > 0$, $P_2 > 0$, $P_3 > 0$, $P_4 > 0$ and $P_5 > 0$ if S_h, S_v, I_h, $I_v > 0$. From Equation (8), it is also clear that S_h, S_v, I_h, and I_v are favorable if $R_0 > 1$. The virus's endemic point of equilibrium E^* is therefore stable locally for $R_0 > 1$ according to the Routh–Hurwitz stable criteria.

5. Estimation of the model's parameters

In this section, we use malaria incidence data collected by the National Malaria Control Program (NMCP) from 2010 to 2022 to estimate the model parameters. Table 1 presents parameter values used to fully parameterize the simulation of malaria transmission from mosquitoes to humans. The remaining parameters were determined using the least-square fitting method, which involves minimizing the error between the model (3) solution and the observed malaria incidence data from 2010 to 2022 (refer to Figure 2). The multi-start approach with 1000 points of departure was used to fit the model in the MATLAB computer language. The following objective function is employed in the parameter estimation:

$$\hat{\theta} = \operatorname{argmin} \sum_{i=1}^{n} \left(\beta_h L_h - \text{data}_{t_i}\right)^2 \quad (14)$$

where data_{t_l} represents the model solution at the time $t_i$and the malaria incidence data and n are the number of available data points. Table 1 tabulates the model's associated parameters (3).

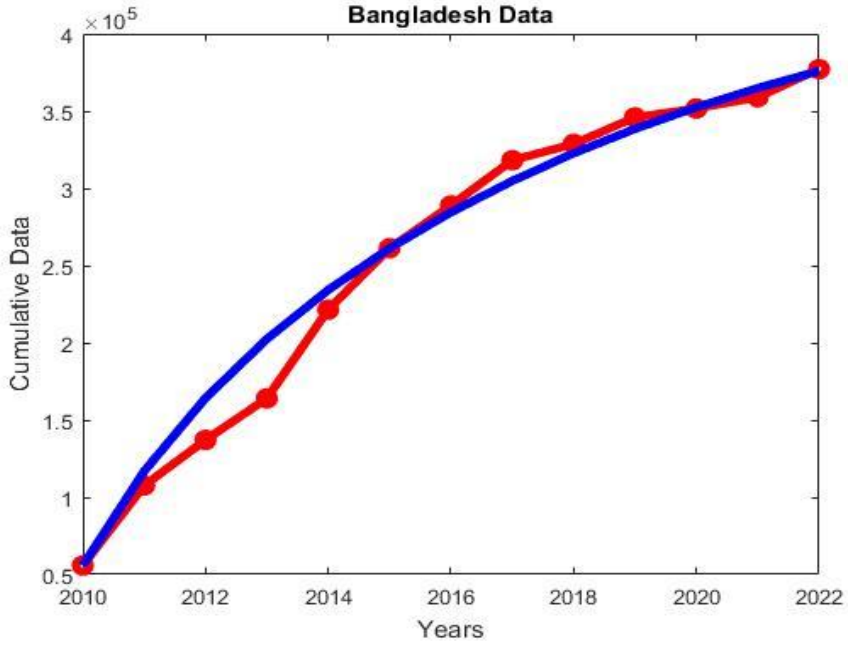

Fig. 2. Data on reported cases of malaria (red dot line) and the associated best fit (blue solid line).

Table 1: Parameter values, signs, potential values, and citations are listed.

Parameter description	Signs	Value	Citations
Human population in 2020	N_h	164689383	[36]
Mosquito population	N_v	19080000	[37]
Human birth or death rates per capita	μ_h	0.0095	Variable
Mosquitos birth or death rates per capita	μ_v	0.0085	Variable
The likelihood of infection in humans	β_h	0.0506	Fitted
The likelihood of infection in mosquitos	β_v	0.0506	Fitted
Human progression rate from I_h to R_h	ω	0.35	Variable
Human mortality rate due to illness	δ_h	0.095	Variable
Mosquito mortality rate due to illness	δ_v	0.12	Variable
Rate of deterioration of human immunity	γ	0.45	Variable

6. Sensitive Analysis

Sensitivity indices are computed to identify key parameters influencing malaria transmission. The results indicate that human-to-mosquito and mosquito-to-human transmission rates, as well as immunity loss, have the most significant impact on R_o. This process helps devise effective management strategies and prevents inaccurate public health predictions. Additionally, sensitivity analysis highlights areas requiring further research to enhance the model's predictive accuracy. For disease transmission modeling, it serves as a valuable tool for developing control strategies and improving public health outcomes. In this section, using the parameter values from Table 2, we assess the sensitivity indices for the basic reproduction numbers (R_{ov} for mosquitoes and R_{oh} for humans). By analyzing two factors influencing disease transmission, our study aims to determine whether the malaria epidemic will persist or eventually fade. The sensitivity index assesses the relationship between key parameters and disease transmission among susceptible individuals, thus helping in the development of policies to mitigate the spread of malaria. The mathematical expression below can be used to represent the sensitivity index of the basic reproduction number in relation to the involved parameters.

$$S_{\beta_h} = \frac{\partial R_{oh}}{\partial \beta_h} \frac{\beta_h}{R_{oh}} \tag{15}$$

The parameters involved in the calculation of the fundamental reproduction numbers R_{oh} and R_{ov} are represented by β_i in this case.

Table 2. Sensitivity indices to the parameters for the model

Parameter	Sensitivity index (R_{oh})	Parameter	Sensitivity index (R_{ov})
β_h	+1	β_v	+1
δ_h	-0.20902	δ_v	-0.93385
ω	-0.77008	μ_v	-0.51477
μ_h	-0.04599		

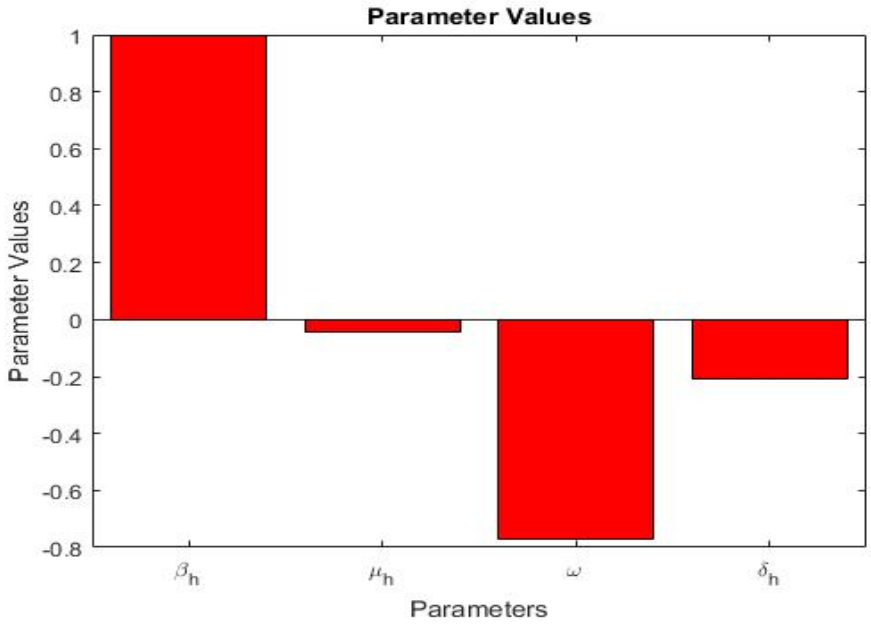

Fig.3. Bar chart depicting the sensitivities indices of the model output o f basic reproduction number $R_{0h}$with respect to the estimated parameters β_h, μ_h, ω, δ_h.

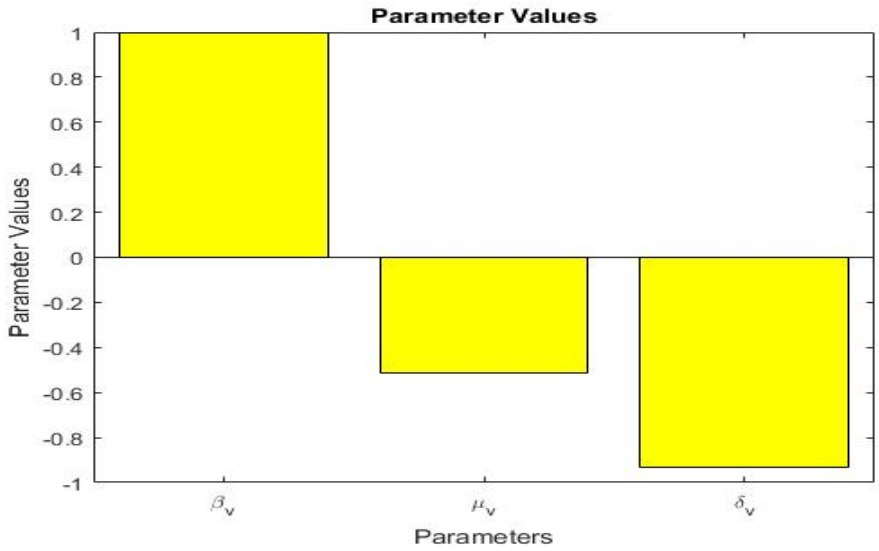

Fig.4. Bar chart depicting the sensitivities indices of the model output of basic reproduction number $R_{0v}$with respect to the estimated parameters β_v, μ_v, δ_h.

Figure 3 illustrates that the parameter β_h has a vital part in increasing the infectious state of humans (I_h*), while the parameters μ_h, ω, and δ_h significantly contribute to reducing this state. Likewise, as illustrated in Figure 4, the parameter β_v is instrumental in the spread of the infectious state in mosquitoes (I_v*). Conversely, parameters such as μ_v and δ_v help decrease the number of infectious states.

7. Bifurcation Analysis

Bifurcation analysis is conducted to examine how parameter variations affect disease stability. Forward bifurcations are observed, indicating that a reduction in transmission rates below a critical threshold ensures malaria eradication.

The bifurcation analysis of the system described in Equations (3) is discussed both mathematically and graphically here.

Theorem 7.1: The proposed model Equations (3) has forward bifurcation at $\beta_h = \beta_h^*$ at $R_0 = 1$, whenever a < 0.

Proof: Consider $S_h = x_1$ and similarly, $I_h = x_2$, $R_h = x_3$, $S_v = x_4$, $I_v = x_5$. Then the system described in (3), can be written as

$$\begin{aligned}
\frac{dx_1}{dt} &= f_1 = \mu_h N_h + \gamma x_3 - \beta_h x_1 x_5 - \mu_h x_1 \\
\frac{dI_h}{dt} &= f_2 = \beta_h x_1 x_5 - (\omega + \delta_h + \mu_h) x_2 \\
\frac{dR_h}{dt} &= f_3 = \omega x_2 - (\gamma + \mu_h) x_3 \\
\frac{dS_v}{dt} &= f_4 = \mu_v N_v - \beta_v x_4 x_2 - \mu_v x_4 \\
\frac{dI_v}{dt} &= f^5 = \beta_v x_4 x_2 - (\delta_v + \mu_v) x_5
\end{aligned} \tag{16}$$

The bifurcation parameter is identified as the transmission rate among the susceptible population that has not been vaccinated, with the condition that $R_0 = 1$. Choose $\beta_h = \beta_h^*$ as a bifurcation parameter. Solving for β_h^* from $R_0 = 1$ gives

$$\beta_h^* = \frac{(\delta_v + \mu_v)(\omega + \delta_h + \mu_h)}{N_h \mu_h N_v \mu_v \beta_v}$$

So, the disease-free equilibrium points for the transformed system

$$E^0 = (x_1^0, x_2^0, x_3^0, x_4^0, x_5^0) = (N_h, 0, 0, N_v, 0)$$

The Jacobian matrix of the system (16) evaluated at the disease-free equilibrium E^0 with $\beta_h = \beta_h^*$ is given by

$$J^* = \begin{pmatrix} -\mu_h & 0 & \gamma & 0 & -\beta_h^* N_h \\ 0 & -(\mu_h + \delta_h + \omega) & 0 & 0 & \beta_h^* N_h \\ 0 & \omega & -(\gamma + \mu_h) & 0 & 0 \\ 0 & -\beta_v N_v & 0 & -\mu_v & 0 \\ 0 & \beta_v N_v & 0 & 0 & -(\mu_v + \delta_v) \end{pmatrix}$$

The Jacobian J* of the linearized system has a simple zero eigenvalue with all other eigenvalues having negative real parts. In the scenario of $R_0 = 1$, using the technique [38], it can be shown that the matrix J* has a right eigenvector (corresponding to the zero eigenvalues), given by $w = [w_1 w_2 w_3 w_4 w_5]^T$, where

$w_1 = -\frac{\mu_h^2 + \mu_h(\gamma + \delta_h + \omega) + \gamma\delta_h}{\omega\mu_h} w_3$, $w_3 = w_3 > 0$, $w_2 = \frac{(\gamma + \mu_h)}{\omega} w_3$, $w_4 = -\frac{\beta_v N_v(\gamma + \mu_h)}{\mu_v \omega} w_3$, and $w_5 = \frac{(\mu_h + \delta_h + \omega)(\gamma + \mu_h)}{\omega\beta_h N_h} w_3$.

Similarly, the components of the left eigenvector of J* (corresponding to the zero eigenvalue), denoted by $v = [v_1 v_2 v_3 v_4 v_5]^T$, are given by

$v_1 = v_3 = v_4 = 0$, $v_2 = v_2 > 0$ and $v_5 = \frac{\beta_h^* N_h}{(\mu_v + \delta_v)} v_2$.

So, the bifurcation coefficients a and b are

$$a = \sum_{m,n,l=1}^{5} v_l w_m w_n \frac{\partial^2 f_l}{\partial x_m \partial x_n}$$

$$= -\frac{\beta_v N_v(\mu_h + \delta_h + \omega)(\gamma + \mu_h)^2}{\mu_h N_h \mu_v^2 \omega^2} \left[\frac{\mu_v^2 N_v \beta_h \{\mu_h(\mu_h + \delta_h + \omega) + \gamma(\gamma + \mu_h)\}}{(\mu_h + \delta_h + \omega)(\gamma + \mu_h)(\mu_v + \delta_v)} + R_0^2 \right]$$

and $b = \sum_{i,k=1}^{5} v_k w_i \frac{\partial^2 f_k}{\partial x_i \partial \beta} = \beta_h^* v_2 w_5 > 0$.

After computing the partial derivative of the modified function (), inserting the associated rate values for the parameters, and substituting the appropriate values of $w = (w_1, w_2, w_3, w_4, w_5)$ and $v = (v_1, v_2, v_3, v_4, v_5)$, we notice the forward bifurcation at $R_0 = 1$. When $R_0 > 1$, the forward bifurcation situation has an unstable disease-free equilibrium and a stable disease-endemic equilibrium point (see Figure 5). The bifurcation parameter is identified as the transmission rate among the susceptible population, with the condition that $R_0 = 1$.

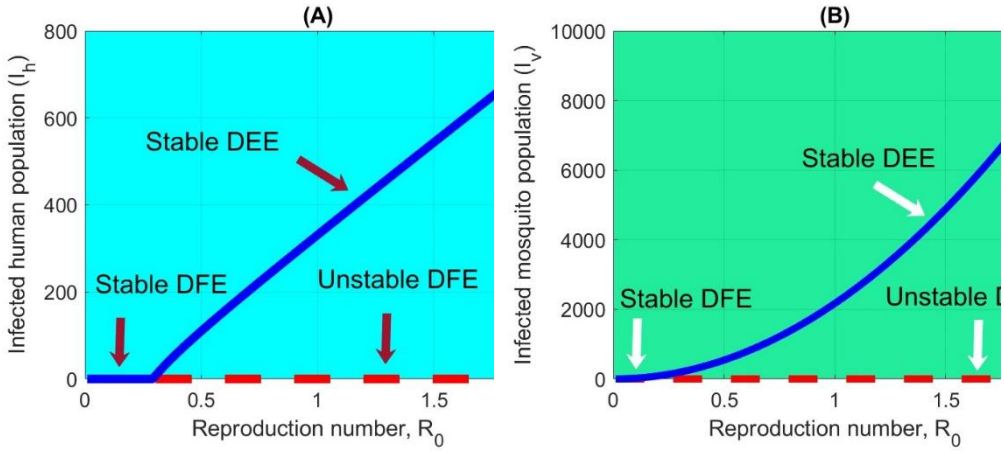

Fig. 5. A bifurcation graphic that illustrates how the stability of R_0 improves as R_0 goes from 0 to 2.

Bifurcation analysis explores how the system's behavior changes with variations in the basic reproduction number R_0. Our malaria model helps identify the point at which the system transitions from an endemic state to a disease-free state. When $R_0 < 1$, the system is in a stable disease-free equilibrium, meaning malaria will eventually disappear. Conversely, when R_0 exceeds 1, the system reaches an endemic equilibrium, where the disease persists. This analysis highlights the importance of keeping R_0 below 1 for malaria eradication, as values above 1 lead to continuous transmission.

Theorem 7.2: Consider the malaria transmission model described by the system (16), where R_0 is the basic reproduction number and β_v is the mosquito-to-human transmission rate. At the critical value $\beta_v = \beta_v^*$, corresponding to $R_0 = 1$, the disease-free equilibrium (DFE) undergoes a bifurcation.

If the bifurcation coefficients $a < 0$ and $b > 0$, the following conclusions can be drawn:

1. For $R_0 < 1$, the DFE is locally asymptotically stable, and no endemic equilibrium exists.
2. For $R_0 > 1$, the DFE becomes unstable, and a unique stable endemic equilibrium emerges.

This behavior indicates that the system exhibits a forward bifurcation, where the stability of the DFE changes at $R_0 = 1$, and the endemic equilibrium smoothly branches off as R_0 increases beyond 1.

Proof: Given $R_0 = 1$, solve for the critical value of $\beta_v = \beta_v^*$ in terms of the model parameters:

$$\beta_v^* = \frac{(\delta_v + \mu_v)(\omega + \delta_h + \mu_h)}{N_h \mu_h N_v \mu_v \beta_v}$$

The Jacobian matrix J^* of the system evaluated at E^0 with $\beta_v = \beta_v^*$ is:

$$J^* = \begin{pmatrix} -\mu_h & 0 & \gamma & 0 & -\beta_h N_h \\ 0 & -(\mu_h + \delta_h + \omega) & 0 & 0 & \beta_h N_h \\ 0 & \omega & -(\gamma + \mu_h) & 0 & 0 \\ 0 & -\beta_v^* N_v & 0 & -\mu_v & 0 \\ 0 & \beta_v^* N_v & 0 & 0 & -(\mu_v + \delta_v) \end{pmatrix}$$

This matrix has a simple zero eigenvalue, with all other eigenvalues having negative real parts at $R_0 = 1$.

Using the Castillo-Chavez and Song methodology, compute the eigenvectors associated with the zero eigenvalue.

Right eigenvector $w = [w_1, w_2, w_3, w_4, w_5]^T$:

$w_1 = -\frac{\mu_h^2 + \mu_h(\gamma + \delta_h + \omega) + \gamma\delta_h}{\omega\mu_h} w_3$, $w_3 = w_3 > 0$, $w_2 = \frac{(\gamma + \mu_h)}{\omega} w_3$,

$w_4 = -\frac{\beta_v^* N_v(\gamma + \mu_h)}{\mu_v \omega} w_3$, and $w_5 = \frac{(\mu_h + \delta_h + \omega)(\gamma + \mu_h)}{\omega \beta_h N_h} w_3$.

Left eigenvector $v = [v_1, v_2, v_3, v_4, v_5]^T$:

$v_1 = v_3 = v_4 = 0$, $v_2 = v_2 > 0$ and $v_5 = \frac{\beta_h N_h}{(\mu_v + \delta_v)} v_2$.

The coefficient a is given by

$$a = \sum_{m,n,l=1}^{5} v_l w_m w_n \frac{\partial^2 f_l}{\partial x_m \partial x_n}$$

After substituting expressions for v, w, and second derivatives of f_l, we find:

$$a = -\frac{\beta_h(\mu_v + \delta_v)(\mu_h + \delta_h + \omega)(\gamma + \mu_h)^2}{\mu_h N_h \mu_v^2 \omega^2} \left[\frac{\mu_v^2 N_v \beta_v^* (\mu_h + \delta_h + \omega) + \gamma(\gamma + \mu_h)}{(\mu_h + \delta_h + \omega)(\gamma + \mu_h)(\mu_v + \delta_v)} + R_0^2 \right].$$

Since a < 0, the bifurcation is forward.

The coefficient b is given by:

$$b = \sum_{i,k=1}^{5} v_k w_i \frac{\partial^2 f_k}{\partial x_i \partial \beta}$$

After substituting the appropriate terms:

$b = \beta_v^* v_2 w_5 > 0$

8. Numerical Simulations

This section presents the application of the proposed model, using specified initial conditions, to perform numerical simulations and visualize the dynamics of disease transmission. The simulation aims to support decision-making and investigate how various control strategies can mitigate the transmission of infectious diseases, specifically malaria, in Bangladesh. We perform a comprehensive numerical analysis using the ODE45 solver in MATLAB, which validates the analytical findings and assesses the effects of key factors such as immunity loss, human infection rate, recovery rate, and disease-induced mortality on malaria incidence. We used various initial conditions for each population to evaluate the stability of the model's equilibrium points. The model suggests that malaria will gradually disappear from the population if the basic reproduction number, R_0, is less than 1. However, if R_0 is greater than 1, malaria will persist in the population. We compared the human-infected population with the mosquito-infected population by applying several initial conditions to the system. The parameter values used in the numerical simulations were taken from Table 1. These methods allow us to solve the model and obtain the desired results.

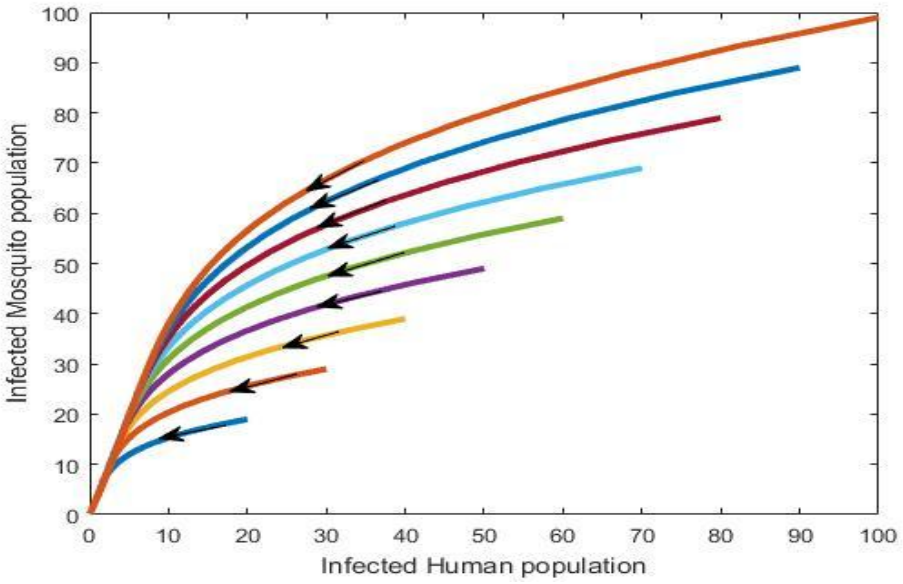

Fig. 6. Relationship between infected Mosquito population vs Human population when $R_0 < 1$.

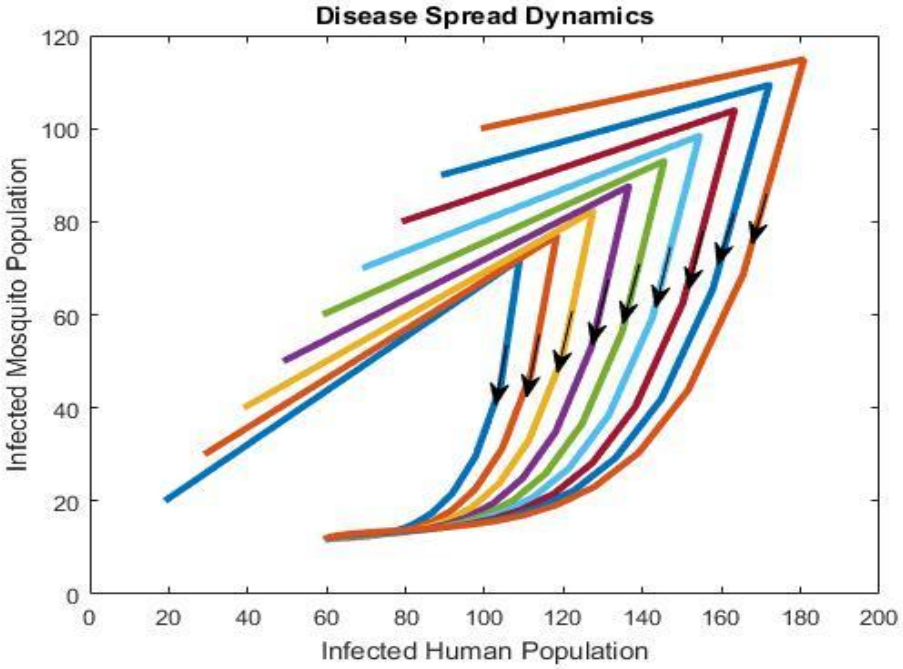

Fig. 7. Relationship between infected Mosquito population vs Human population when $R_0 > 1$.

The trajectories of the model, using various initial values for all compartmental variables, are depicted in Figures 6 and 7, which illustrate the transmission patterns for both the disease-free and endemic equilibria. In Figure 6, the disease transmission gradually declines to zero, as the trajectories converge to the disease-free equilibrium point, signifying that the disease will fade out from the population when $R_0 < 1$. In contrast, Figure 7 highlights the progression of the disease under endemic conditions for $R_0 > 1$. The trajectories stabilize at positive values for both infected human and mosquito populations, demonstrating the persistence of the disease within the population. This figure shows how, in the context of a high transmission rate, the infectious agent spreads and stabilizes, maintaining endemicity over time. This study presents malaria incidence alongside various rate factors and the basic reproduction number (R_0). In, prevalence refers to the proportion of individuals in the population who are infected at a given time. Monitoring this prevalence is crucial for tracking the spread of the disease and informing public health strategies aimed at controlling and preventing further transmission.

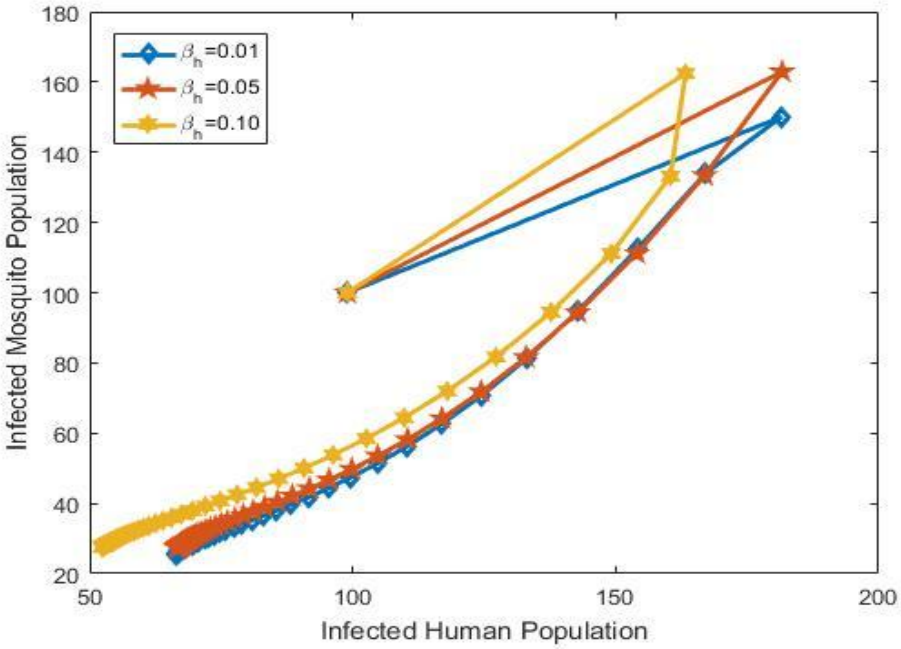

Fig. 8. The behaviour of infected humans for the different values of transmission rate (β_h) when R_0 >1.

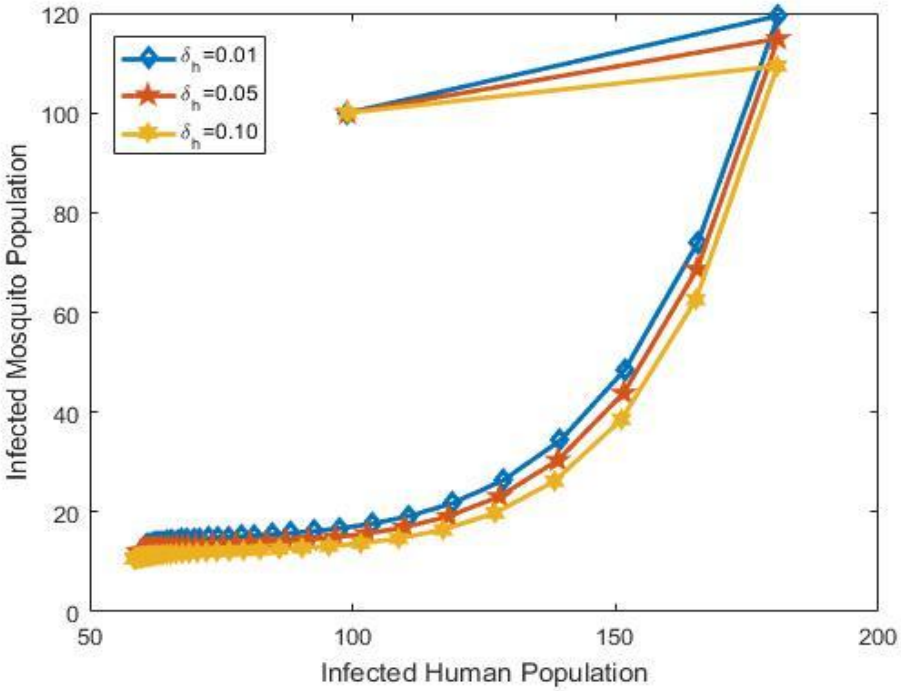

Fig. 9. The behaviour of infected humans for the different values of disease-related death rate(δ_h) when R_0 > 1.

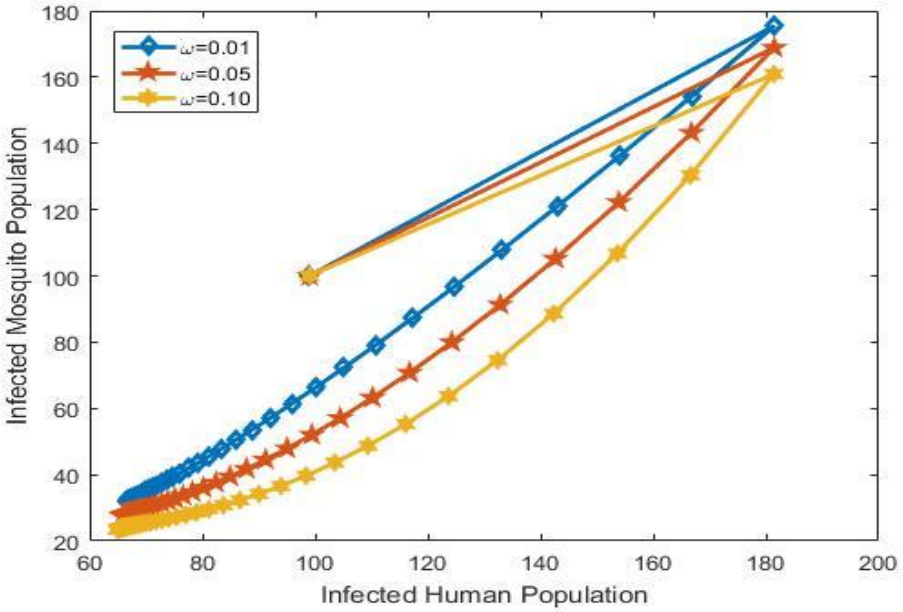

Fig. 10. The behavior of infected humans for the different values of recovery rate (ω) when $R_0 > 1$.

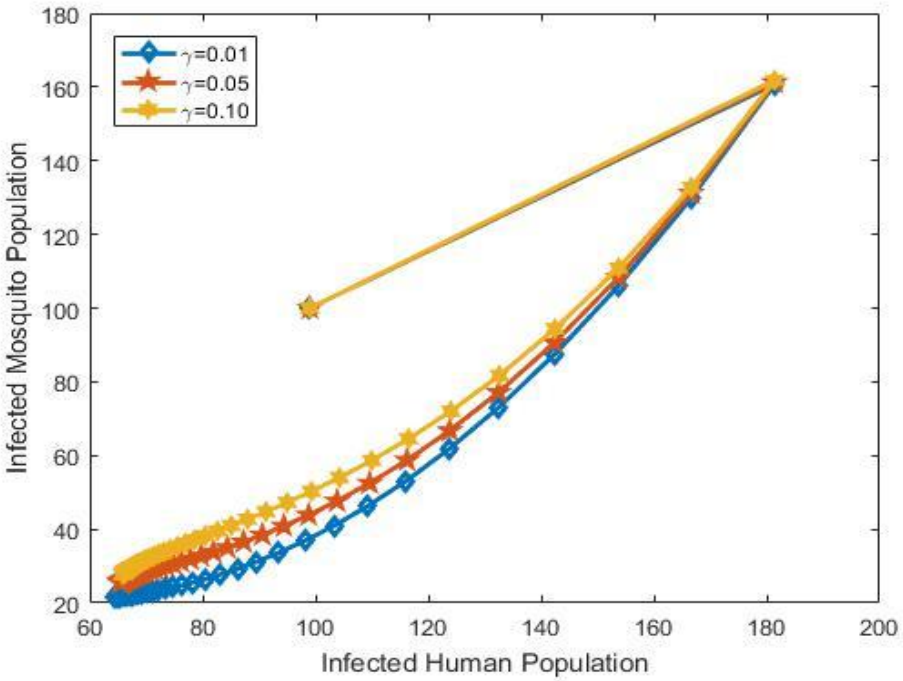

Fig. 11. The behaviour of infected humans for the different values of loss of immunity(γ) when $R_0 > 1$.

Figures 8–11 illustrate the system's behavior under various model parameter values. By keeping the other parameters from Table 1 constant and ensuring that the basic reproduction number is greater than one, Figures 8 and 9 demonstrate how changes in the transmission rate and disease-related mortality rate impact the infected population. Specifically, Figure 8 indicates that an increase in the transmission rate (β_h) is associated with a higher prevalence of malaria. In contrast, Figure 9 shows that an increase in the disease-related mortality rate (δ_h) reduces overall malaria prevalence. This study highlights the importance of managing the rate of disease spread to effectively implement various intervention strategies, including public awareness campaigns, diagnostic initiatives, and health education programs. Figures 10 and 11 illustrate the effects of the recovery rate (ω) and loss of immunity (γ) on the human population. The computational models presented in Fig. 10 indicate that an increase in the recovery rate (ω) leads to a decrease in infected individuals. Conversely, Figure 11 shows that a decline in the immunity rate (γ) increases the infected population. Implementing intervention strategies, such as timely medical treatment, transfeminine-based combination therapy, and measures to prevent chronic infections, is expected to reduce human infections and enhance recovery rates. Therefore, lowering the transmission rate is essential for executing different intervention strategies, including public awareness campaigns, diagnostic programs, and health education initiatives.

9. Discussion and Conclusion

Malaria is a severe global health threat, with millions affected worldwide, particularly in low- and middle-income regions such as sub-Saharan Africa and parts of South Asia. Despite global efforts for control and elimination, malaria remains a leading cause of morbidity and mortality, placing a considerable burden on healthcare systems and affecting economic growth. Vulnerable groups, including young children and pregnant women, are disproportionately impacted. Understanding malaria transmission dynamics is critical to developing effective strategies for reducing its global burden, as this disease continues to hinder socio-economic progress in affected regions.

Malaria significantly impacts health, education, and economic development in endemic areas. The disease's burden extends beyond immediate health effects, as recurrent infections impede cognitive development in children, limit educational attainment, and reduce workforce productivity, leading to substantial economic costs for families and communities. Malaria also overwhelms healthcare facilities, especially in rural regions with limited resources, further emphasizing the need for effective control strategies to break the cycle of poverty and illness in affected populations.

In Bangladesh, malaria remains a prominent public health issue, particularly in hilly and border areas like the Chattogram Hill Tracts, Sylhet, and Mymensingh. These regions, characterized by dense forests and conducive environmental

conditions, are highly susceptible to transmission. Limited healthcare access in these marginalized communities exacerbates malaria's effects, increasing mortality and complicating efforts to control outbreaks. Cross-border population movement and regional ecological factors further challenge containment efforts, underscoring the importance of a coordinated, region-specific approach to malaria control in Bangladesh.

In this study, we developed and analyzed a compartmental model to represent the non-linear dynamics of malaria transmission between humans and mosquitoes. The proposed model categorizes humans into susceptible, infectious, and recovered groups, while mosquitoes are classified as susceptible or infectious, as they remain infected for life. By incorporating non-linear forces of infection with saturated incidence rates, model results differed from traditional models, which typically employed standard incidence rates or basic mass-action approaches. The results of the model were validated both epidemiologically and mathematically for a specific region, with a disease-free equilibrium point identified.

Our findings underscore the critical role of the basic reproduction number (R_0) in determining malaria dynamics, consistent with previous studies [1, 2]. Similar to the work of Gebremeskel et al. (2023) [41], our bifurcation analysis highlights the importance of maintaining $R_0 < 1$ to achieve malaria eradication. Moreover, the sensitivity analysis confirms that targeted interventions, such as those outlined by Asamoah et al. (2022) [42], can significantly reduce transmission rates and disease prevalence. These results reinforce the value of mathematical modeling in guiding public health strategies and contribute to the growing body of research emphasizing the interplay between transmission dynamics and control measures in endemic regions.

Our model aims to encourage future researchers to explore natural treatments for reducing malaria transmission, devise strategies for local and national malaria control, and enhance public awareness of prevention methods. Public health education and social media campaigns can play a critical role in fostering effective community engagement to combat malaria. Furthermore, policy options addressing environmental and socioeconomic factors could contribute to more sustainable solutions for malaria control and elimination in Bangladesh and comparable regions.

References

[1] Mendis K, Sina BJ, Marchesini P, Carter R. 2001. The neglected burden of Plasmodium vivax malaria. Am. J. Trop. Med. Hyg. 64:97–106.

[2] Guerra CA, Howes RE, Patil AP, Gething PW, Van Boeckel TP, Temperley WH, Kabaria CW, Tatem AJ, Manh BH, Elyazar IR, Baird JK, Snow RW, Hay SI. 2010. The international limits and population at risk of

Plasmodium vivax transmission in 2009. PLoSNegl. Trop. Dis. 4:e774 doi:10.1371/journal.pntd.0000774.

[3] J. Liu-Helmersson, H. Stenlund, and A. Wilder-Smith et al, Vectorial capacity of Aedesaegypti: effects of temperature and implications for global dengue epidemic potential, Addison-Wesley Publishing Company, PloS one 9 (2014), e89783.

[4] K. L. Gage, T. R. Burkot, and R. J. Eisen et al, Climate and vector borne diseases, American journal of preventive medicine (2008).

[5] The *P. vivax* information hub, vivaxmalaria.org , World Malaria Report 2022.

[6] A. Rahman, M.A. Kuddus, Cost-effective modeling of the transmission dynamics of malaria: A case study in Bangladesh, communications in statistics: Case studies, Data Anal. Appl. (2020) 1–17.

[7] KoellaJ.C. On the use of mathematical models of malaria transmission Acta Tropica, 1991.

[8] Tilahun GT, Demie S, Eyob A. Stochastic Model of measles transmission dynamics with double dose vaccination. Infect Dis Model 2020; 5:478-94.

[9] Kermack, W. O. and A. G. McKendrick, 1991a. Contributions to the mathematical theory of epidemics - I. Bulletin of Mathematical Biology, 53:33–55.

[10] Kermack, W. O. and A. G. McKendrick, 1991b. Contributions to the mathematical theory of epidemics II. Bulletin of Mathematical Biology, 53:57–87.

[11] Kermack, W. O. and A. G. McKendrick, 1991c. Contributions to the mathematical theory of epidemics III. Bulletin of Mathematical Biology, 53:89–118.

[12] Li Y., Liu X. Modeling and control of mosquito-borne diseases with Wolbachia and insecticides. Theoretical Population Biology. 2020;132(1):82–91.

[13] Marshall J.M., Wu S.L., Kiware S.S., Ndhlovu M., Ouédraogo A.L., Touré M.B., Sturrock H.J., Ghani A.C., Ferguson N.M. Mathematical models of human mobility of relevance to malaria transmission in Africa. Scientific Reports. 2018;8(1):1–2.

[14] Sweilam N.H., Al-Mekhlafi S.M., Mohammed Z.N., Baleanu D. Optimal control for variable order fractional HIV/AIDS and malaria mathematical models with multi-time delay. Alexandria Engineering Journal. 2020;59(5):3149–3162.

[15] Awine T., Malm K., Bart-Plange C., Silal S.P. Towards malaria control and elimination in Ghana: Challenges and decision-making tools to guide planning. Global Health Action. 2017;10(1).

[16] Almeida R., Martins N., Silva C.J. Global stability condition for the disease-free equilibrium point of fractional epidemiological models. Axioms. 2021;10(4):238.

[17] Edeki S.O., Adinya I., Adeosun M.E., Ezekiel I.D. Mathematical analysis of the global COVID-19 spread in Nigeria and Spain based on SEIRD model. Commun. Math. Biol. Neurosci. 2020;84(1):1–10.

[18] Handari B.D., Amalia A., Rahmayani A.S., Aldila D. Numerical simulation of malaria transmission model considering secondary infection. Commun. Math. Biol. Neurosci. 2020;36(1):1–10.

[19] Tchoumi S.Y., Kouakep Y.T., Fotsa D.J., Kamba F.G., Kamgang J.C., Houpa D.D. Mathematical model for acquiring immunity to malaria: A PDE approach. Bio-Mathematics. 2021;10(2).

[20] Singh S. et al. 2005. Modelling and Analysis of The Spread of Malaria: Environmental and Ecological Effects. Journal of Biological Systems. 13(01): 1-12.

[21] Zwerling A, Shrestha S, Dowdy DW. Mathematical Modelling and Tuberculosis: Advances in Diagnostics and Novel Therapies. Advances in Medicine 2015; 2015:10.

[22] Bacaër N, Ouifki R, Pretorius C, Wood R, Williams B. Modeling the joint epidemics of TB and HIV in a South African township. Journal of Mathematical Biology 2008; 57(4):557.

[23] Liu L, Zhao X-Q, Zhou Y. A Tuberculosis Model with Seasonality. Bulletin of Mathematical Biology 2010; 72(4):931–52.

[24] Blaser N, Zahnd C, Hermans S, Salazar-Vizcaya L, Estill J, Morrow C, Egger M, Keiser O, Wood R. Tuberculosis in Cape Town: An age-structured transmission model. Epidemics 2016; 14:54–61.

[25] Guzzetta G, Ajelli M, Yang Z, Merler S, Furlanello C, Kirschner D. Modeling socio-demography to capture tuberculosis transmission dynamics in a low burden setting. Journal of theoretical biology 2011; 289:197–205.

[26] Childs LM, Abuelezam NN, Dye C, Gupta S, Murray MB, Williams BG, Buckee CO. modelling challenges in context: Lessons from malaria, HIV, and tuberculosis. Epidemics 2015; 10:102–7.

[27] Jajarmi A, Yusuf A, Baleanu D, Inc M. A new fractional HRSV model and its optimal control: a non-singular operator approach. Physica A: Statistical Mechanics and its Applications 2020; 547:123860.

[28] Mustapha UT, Qureshi S, Yusuf A, Hincal E. Fractional modeling for the spread of Hookworm infection under Caputo operator. Chaos, Solitons & Fractals 2020; 137:109878.

[29] Kuddus MA, Meehan MT, White LJ, McBryde ES, Adekunle AI. Modeling drug-resistant tuberculosis amplification rates and intervention strategies in Bangladesh. Plos one 2020; 15(7): e0236112.

[30] D. Khamis, C. El Mouden, K. Kura, M.B. Bonsall, Optimal control of malaria: combining vector interventions and drug therapies, Malar. J. 17 (1) (2018) 174.

[31] O. Koutou, B. Traoré, B. Sangaré, Mathematical modeling of malaria transmission global dynamics: taking into account the immature stages of the vectors, Adv. Difference Equ. 2018 (1) (2018) 220.

[32] N. Chitnis, J.M. Hyman, C.A. Manore, Modelling vertical transmission in vector-borne diseases with applications to Rift Valley fever, J. Biol. Dyn. 7 (1) (2013) 11–40.

[33] A.A. Lashari, S. Aly, K. Hattaf, G. Zaman, I.H. Jung, X.-Z. Li, Presentation of malaria epidemics using multiple optimal controls, J. Appl. Math. 2012 (2012).

[34] J.D. Murray, Mathematical Biology: I. An Introduction, Springer Science & Business Media, 2007.

[35] A.D. Polyanin, A.V. Manzhirov, Handbook of Mathematics for Engineers and Scientists, CRC Press, 2006.

[36] The World Bank, https://datacatalog.worldbank.org/dataset/world-development-indicators/.

[37]J.K.K. Asamoah, F. Nyabadza, Z. Jin, E. Bonyah, M.A. Khan, M.Y. Li, T. Hayat, Backward bifurcation and sensitivity analysis for bacterial meningitis transmission dynamics with a nonlinear recovery rate, Chaos, Solit. Fractals 140 (2020) 110237.

[38] S. Athithan, M. Ghosh, Stability analysis and optimal control of a malaria model with larvivorous fish as biological control agent, Appl. Math. Inform. Sci. 9 (4) (2015) 1893.

[39] A.A. Gebremeskel, Global stability of malaria transmission dynamics model with logistic growth, Discrete Dyn. Nat. Soc. 2018 (2018).

[40] H.-F. Huo, G.-M. Qiu, Stability of a mathematical model of malaria transmission with relapse, in: Abstract and Applied Analysis, Hindawi, 2014.

[41] Gebremeskel, H. et al. 2023. Dynamics of vector-borne diseases: Modeling and control measures in malaria-endemic regions. Journal of Theoretical Biology, 542:110897.

[42] Asamoah, J.K.K. et al. 2022. Backward bifurcation and sensitivity analysis for bacterial meningitis transmission dynamics with a nonlinear recovery rate. Chaos, Solitons & Fractals, 140:110237.